Electronic Supplementary Information

A novel catalytic heme cofactor in SfmD with a single thioether bond and a *bis*-His ligand set revealed by a *de novo* crystal structural and spectroscopic study

Inchul Shin[a], Ian Davis[a], Karinel Nieves-Merced[a,b], Yifan Wang[a], Stanton McHardy[a,b], and Aimin Liu[a,*]

[a]Department of Chemistry and [b]Center for Innovative Drug Discovery, The University of Texas at San Antonio, Texas 78249, United States

*To whom correspondence should be addressed:
Aimin Liu, E-mail: Feradical@utsa.edu

Supplementary Information video clip caption:

A 19-s video clip (http://www.rsc.org/suppdata/d0/sc/d0sc06369j/d0sc06369j1.mp4) showing the transition between the resting state (6VDQ.pdb) and the partially reduced state (6VE0.pdb) from three different viewing angles. The video is presented in the mp4 format with a frame rate of 30 frames/second and in the Full HD (1920×1080 pixel) resolution.

Contents

Materials and Methods

Synthesis and characterization of 3-Me-L-Tyr

The synthesis of the title compound, 3-Me-L-Tyr, was completed following conditions previously described in the literature.[1, 2] Two minor modifications were employed in the published syntheses; 1) THF was used instead of DMF in step d, and 2) a solution of sodium bicarbonate was not used for the purification of the final product, affording the TFA salt directly.

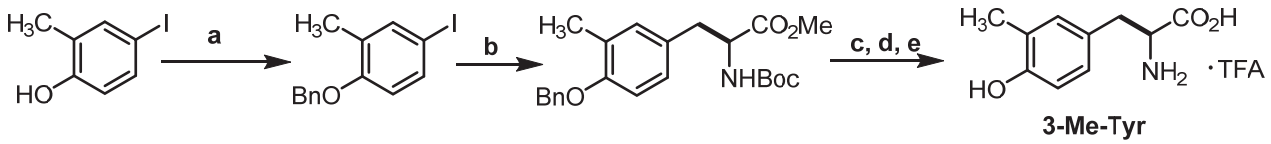

Reagents and Conditions: a) benzylbromide, K_2CO_3, Acetone, 96%; b) methyl (*R*)-2-((*tert*-butoxycarbonyl)amino)-3-iodopropanoate, Zn, $Pd_2(dba)_3$, DMF, 42%; c) $Pd(OH)_2$/C, MeOH, 98%; d) LiOH, THF, water, 80%; e) TFA, DCM, 71%.

<u>Experimental description for modified steps</u>

Saponification (step d):

To a solution of methyl ester (120 mg, 0.388 mmol) in THF (2.8 mL) was added H_2O (0.92 mL) and LiOH (18.6 mg, 0.777 mmol). The reaction mixture was stirred for 2 h at rt. The reaction mixture was quenched with 1.0 M HCl until pH ~2 and extracted with EtOAc (×2). The organic phase was concentrated and dried under reduced pressure. The crude material was purified by flash-chromatography eluting with 0-50% gradient of methanol in DCM.

Amine deprotection (step e):

To a solution of Boc-amino acid (90 mg, 0.305 mmol) in DCM (2.9 mL) was added TFA (2.0 mL). The reaction mixture was stirred for 2 h at rt. The reaction mixture was concentrated and dried under reduced pressure. The crude material was lyophilized with celite and purified by flash-chromatography C18 eluting with a 0-5% gradient of acetonitrile in water.

The synthesis above yielded (S)-2-amino-3-(4-hydroxy-3-methylphenyl)propanoic acid (3-Me-L-Tyr) as a white solid; ^{1}H NMR (400 MHz, D_2O) δ 6.97 (s, 1H), 6.89 (d, *J* = 8.0 Hz, 1H), 6.74 (d, *J* = 8.0 Hz, 1H), 3.80 (m, 1H), 3.05 (dd, *J* = 5.3, 15.1 Hz, 1H), 2.89 (dd, *J* = 8.0, 15.1 Hz, 1H), 2.08 (s, 1H); ^{13}C NMR (100 MHz, D_2O) δ 174.0, 152.9, 132.0, 127.9, 126.9, 125.5, 115.4, 56.0, 35.4, 15.1; ^{19}F NMR (400 MHz, D_2O) δ -75.6; HR-MS calcd for $C_{10}H_{14}NO_3^+$ 196.0968, found 196.0972.

<u>Enantiopurity determination</u>

The synthesis of methyl (*S*)-2-amino-3-(4-(benzyloxy)-3-methylphenyl)propanoate Mosher amide for enantiopurity investigation was completed following similar conditions previously described in the literature.[3]

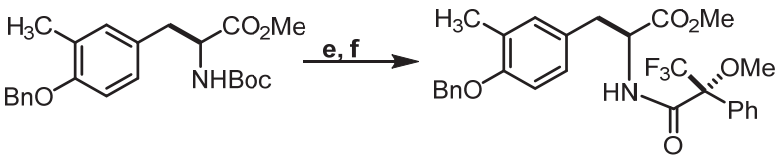

Reagents and Conditions: e) TFA, DCM; f) (*S*)-(+)-MTBA-Cl, TEA, DCM

The Boc group of methyl (*S*)-3-(4-(benzyloxy)-3-methylphenyl)-2-((*tert*-butoxycarbonyl)amino)propa-noate intermediate was removed following the previously described step e to generate the amine. Then, to a solution of amine (17.2 mg, 0.057 mmol) and TEA (37.6 µL, 0.27 mmol) in DCM (1 mL) was added (*S*)-(+)-Mosher's acid chloride (11.8 µL, 0.063 mmol) as a solution in DCM (1 mL). The solution was stirred until complete consumption of starting material was observed by TLC and HPLC/MS (10 minutes) and filtered through a silica gel plug (pipette column with DCM) and concentrated under reduced pressure to generate methyl (*S*)-2-amino-3-(4-(benzyloxy)-3-methylphenyl)propanoate Mosher amide as colorless oil in ≥98% ee. The % ee was determined by ^{1}H-NMR, and no trace of the other enantiomer was observed (Fig. S1).

Cloning, Expression, and Purification

Full-length gene (1 – 365) and a truncated variant (16 – 353) of SfmD from *Streptomyces lavendulae* NRRL 11002 were used in this study. The genes were amplified using sequence-specific primers (Table S2) and DNA template, which was a generous gift from Dr. Gong-Li Tang. The resulting PCR products were digested by NdeI and HindIII restriction enzymes and ligated to a modified pET-28a vector (Merck) in which contains a *Tobacco etch virus* (TEV) protease cleavage site designed for the removal of the N-terminal polyhistidine tag. The DNA sequences of constructed expression vector plasmids were verified by DNA sequencing (Eurofins Genomics). His-tagged SfmD proteins were expressed in *E. coli* BL21 (DE3). Cells were grown in Luria Bertani (LB) media at 37 °C with 220 rpm shaking. When OD_{600} reached 0.3, 160 mg of 5-aminolevulinic acid and 14 mg of ferrous ammonium sulfate were supplemented per Liter of media. The induction of SfmD gene expression was started by adding 0.5 mM isopropyl-L-thio-β-D-galactopyranoside (IPTG) when OD_{600} was between 0.6 and 0.8. The temperature was lowered to 20 °C, and cells were grown for 12 – 16 h. Harvested cells were suspended with 10 mL of buffer A (50 mM Tris-HCl, 200 mM NaCl, 5% glycerol, pH 8.0) per gram of biomass and disrupted by LM-20 cell disruptor (Microfluidics). Cell debris was removed by centrifuge at 30,000 × *g* for 1 hour. The resulting supernatant containing His-tagged SfmD was loaded onto Ni-NTA resin, which had been equilibrated with buffer A. His-tagged SfmD was eluted with buffer B (buffer A + 500 mM imidazole). Desalting and buffer exchange to buffer C (50 mM Tris-HCl, 50 mM NaCl, pH 7.4) were carried out using Sephadex G25 (GE Healthcare). His-tag was removed by treating TEV protease. His-tag removed SfmD was separated and collected by flowing through the Ni-NTA resin. Gel filtration chromatography with Superdex 200 (GE Healthcare) was used as a final polishing step of purification. The fraction containing SfmD protein was collected with isocratic elution using buffer C. For obtaining seleno-L-methionine (SeMet) labeled SfmD, *E. coli* BL21 (DE3) harboring the truncated variant of SfmD was grown in M9 minimal medium. Other procedures are identical, except six amino acid mixtures containing lysine, threonine, phenylalanine, leucine, and valine were added to the cell culture fluid at OD_{600} ~ 0.6 to inhibit endogenous methionine biosynthesis [4]. After 30 min, the SeMet-substituted SfmD was expressed for 20 hours at 20 °C with the supplementation of 0.25 mM SeMet and 0.5 mM IPTG. A codon-optimized full-length SfmD gene was synthesized and purchased from GenScript and used as a template for the mutagenesis to resolve the difficulties in PCR due to high GC contents (Table S3).

Enzyme Reaction

Enzyme reactions were set up using various combinations of 30 μM SfmD, 20 mM ascorbate, 1 mM 3-Me-L-Tyr / or L-Tyr, 1 mM H_2O_2 and 10 μg of catalase from bovine liver (Sigma-Aldrich) in buffer D (150 mM K_2HPO_4/boric acid, pH 10.4) as a normoxic buffer. For the higher concentration of O_2 experiments, oxygen gas was bubbled into the reaction system. For tight control of oxygen, water, buffer D, and enzyme solution were degassed using the Schlenk line connected to inert argon gas and vacuum pump. Degassed solutions were brought into the gloveless anaerobic chamber (Coy Laboratory Products). All reactions were carried out at room temperature.

Kinetic assay of SfmD for substrate L-Tyr was carried out as described previously.[5] The reaction was initiated by adding 4 mM H_2O_2 to the mixture composed of 50 μM enzyme and L-Tyr ranging from 0.2 to 4.8 mM in buffer 100 mM Tris-HCl pH 9.0 at 25 °C. The formation of product L-DOPA was monitored using HPLC. Reaction velocity was plotted against each substrate concentration from triplicate. Kinetic parameters were obtained by sigmoidal nonlinear curve fitting with the following equation in Origin Pro version 8.5 (OriginLab Corporation, Northampton, MA, USA) and reported with standard deviation.

$$v_0 = \frac{V_{\max}[S]^n}{({K_{\text{half}}}^n + [S]^n)}$$

Kinetic assay of SfmD using O_2-saturated buffer and 20 mM sodium ascorbate was carried out with 50 μM enzyme and L-Tyr ranging from 0.2 to 5.6 mM in buffer 100 mM Tris-HCl pH 9.0 at 25 °C. Kinetic parameters were obtained by hyperbolic nonlinear curve fitting using the Origin Pro version 8.5 (OriginLab Corporation, Northampton, MA, USA).

Ascorbate derivatives, including 3-*O*-ethyl-L-ascorbate, 2-*O*-α-D-glucopyranosyl-L-ascorbate, 5,6-isopropylidene-L-ascorbate, and L-ascorbate 2-phosphate were purchased from Tokyo Chemical Industry. L-dehydroascorbate was purchased from ACROS Organics. The final 20 mM of ascorbate derivatives were used in the reaction.

High-Performance Liquid Chromatography (HPLC)

Filtered samples were analyzed using an Ultimate-3000SD HPLC rapid separation system equipped with a photodiode array detector (Thermo Scientific). Samples injected were eluted using the solvent containing 97.5% water, 2.4% acetonitrile and 0.1% FA at the flow rate of 1.0 mL/min. InertSustain C18 column with the particle size of 5 μm and the dimension of 4.6 I.D. × 100 mm (GL Sciences Inc.) was used for the HPLC analysis and sample preparation for further mass spectrometry analysis. For the kinetic assay, ascorbate derivatives, and C317S/A mutant enzyme, Hypersil Gold C18 column with the particle size of 5 μm and the dimension of 4.6 I.D. × 250 mm (Thermo Scientific) was used.

Mass Spectrometry

Mass spectra were collected on a maXis plus quadrupole-time of flight mass spectrometer equipped with an electrospray ionization source (Bruker Daltonics) and operated in the positive ionization mode. Samples were introduced via a syringe pump at a constant flow rate of 3 μL/min. The critical source parameters are summarized as follows: capillary voltage, 3500 V with a set endplate offset of –500 V; nebulizer gas pressure, 0.4 bar; dry gas flow rate, 4.0 L/min; source temperature, 200 °C. Mass spectra were an average of one minute of scans collected at a rate of 1 scan per second in the range of $50 \leq m/z \leq 1500$. Compass Data Analysis software version 4.3 (Bruker Daltonics) was used to process all mass spectra.

Absorption Spectroscopy

The absorption experiments were conducted with 6 μM SfmD, 20 mM ascorbate, and 1 mM 3-Me-L-Tyr or L-Tyr. The samples were prepared anaerobically and contained in the airtight cuvette. UV-vis spectra were recorded by using Lambda 25 spectrophotometer (PerkinElmer). The reciprocal relaxation times were obtained by fitting the data using the following equation in Origin Pro version 8.5 (OriginLab Corporation, Northampton, MA, USA):

$$y = A_1 e^{x/t_1} + A_2 e^{x/t_2} + y_0$$

and the results were reported with standard error.

Electron Paramagnetic Resonance (EPR) Spectroscopy

All EPR experiments were performed with 200 μM SfmD wild-type and 70 μM C317S mutant, 50 mM ascorbate, 2.5 mM 3-Me-L-Tyr or L-tyrosine, and 4 mM •NO-releasing agent, DEA NONOate (Cayman Chemical). EPR samples were prepared inside the anaerobic chamber. Incubation time after the addition was 30 min before freezing in liquid nitrogen. EPR spectra were recorded on a Bruker E560 X-band spectrometer equipped with a cryogen-free 4 K temperature system at 9.4 GHz microwave frequency, a SHQE-W resonator at 100 kHz modulation frequency, 1 mW microwave power, 0.6 mT modulation amplitude at 10 K for the ferric heme samples and 50 K, 0.2 mW microwave power, and 0.3 mT modulation amplitude for the ferrous nitrosyl complex samples.

Pyridine Hemochrome Assay

The heme concentration was determined by pyridine hemochrome assay with ε_{557} = 34 $mM^{-1}cm^{-1}$ for the reduced pyridine hemochromagen.[6]

Heme Reconstitution of C317S and C317A

Hemin chloride was treated to C317S and C317A with the molar ratio of protein:hemin=1:1.5. After one hour of incubation at 4 °C, excess unbound hemin was removed by desalting with Sephadex G-25 (GE Healthcare).

Reduction Potential Measurement

The reduction potential of SfmD was measured by a dye-coupled assay method.[7] Nile blue was selected in this measurement. All materials were anaerobically prepared under O_2-free conditions. Potassium phosphate (100 mM, pH 7.0), Nile Blue (40 μM), SfmD (4 μM), and xanthine (300 μM) were mixed together in the airtight cuvette at room temperature. The spectrum of oxidized forms of Nile Blue and SfmD was recorded using Agilent 8453 UV-vis spectrophotometer equipped with a diode-array detector. The reduction of both Nile Blue and SfmD was initiated by adding 50 nM xanthine oxidase. The resulting spectra were recorded every 10 s for 5 min. To obtain the spectrum of fully reduced forms, 10 mM dithionite was added to the reaction mixture. The ratios of oxidized over reduced forms in terms of protein (410 nm) and dye (635 nm) were obtained from the resulting spectra and plotted. From the linear fitting of data to the Nernst equation with the slope close to 1, Y-intercept was obtained. With the known value of the Nile Blue (-116 mV), the reduction potential of SfmD was calculated.

Crystallization, Data Collection, and Structure Determination

Native or SeMet-labelled SfmD (16 – 353) was concentrated up to 40 mg/mL. Crystal was obtained by the hanging-drop vapor diffusion method at 22 °C. The protein drop (2 µL) was mixed with an equal volume of the crystallization solution containing 0.1 M Tris-HCl (pH 8.5), 0.2 M magnesium chloride, and 16 – 20% (w/v) polyethylene glycol 8,000. Multiwavelength anomalous dispersion data for the SeMet-substituted SfmD were collected to a resolution of 2.2 Å on beamline BL9-2 at Stanford Synchrotron Radiation Lightsource (SSRL) (Table S1). Data with a higher resolution of 2.0 Å were later collected using crystals of native SfmD at the same beamline. X-ray diffraction data were collected at 100 K and processed using the program HKL2000.[8] Ethylene glycol (30% v/v) was used as a cryoprotectant for preventing diffraction data loss due to ice rings. The crystal structure of SfmD was determined using multiwavelength anomalous dispersion data and the software programs SOLVE[9] and RESOLVE[10, 11] for phasing and density modifications, respectively. Model building and refinement were performed using COOT[12] and PHENIX.[13] The full-length SfmD crystals were obtained by the hanging-drop vapor diffusion method at 22 °C. Before setting up crystallization, 3-Me-L-Tyr or L-Tyr (5 mM) was supplemented to the protein solution. The crystal was grown under the condition of 0.2 M magnesium chloride, 0.1 M Tris-HCl (pH 8.5), and 30% (w/v) polyethylene glycol 4,000. In the experiments attempting to obtaining reduced SfmD structure, crystals were soaking with dithionite (350 mM), 3-Me-L-Tyr (5 mM) at room temperature. Single-crystal UV-vis spectra were collected before exposing the crystals to X-ray at SSRL beamline BL9-2. X-ray data collection and structure refinement statistics are summarized in Table 1. The wavelength of 0.97913 Å was used for the data collection of 6VDP, and 0.97946 Å for 6VDP, 6VDZ, and 6VE0. Ramachandran statistics were analyzed using the MolProbity program.[13] No Ramachandran outliers were found. 99.01% of 6VDP, 98.68% of 6VDQ, 96.35% of 6VDZ, and 96.01% of 6VE0 were placed in the favored regions.

The structural figures were prepared using PyMOL (Schrödinger, version 2.3.3). Multiple sequence alignment was carried out using Clustal Omega[14], and the amino acid sequence alignment figure was prepared using ESPript.[15] Structure superposition was carried out using CCP4MG.[16] The movie clip showing the transition from the resting state of SfmD structure to a dithionite soaking intermediate structure was generated by UCSF ChimeraX.[17] For periplasmic signal peptide analysis, SignalP (www.cbs.dtu.dk/services/SignalP) was used. Initial structure prediction with the primary sequence of SfmD was performed using Phyre2 server.[18]

Structural Alignment Using the DALI Server

A structural alignment analysis was conducted using the DALI server.[19] The ordered region (18 – 321) of SfmD fetched TDO from *Xanthomonas campestris* (XcTDO, PDB code-chain id, 3BK9-B) with a Z-score of 7.0, sequence identity of 7% and an rmsd value of 2.9 Å. When the C-terminal half of SfmD (180 – 321) is provided, DALI analysis returned the following results: hIDO1 (PDB code-chain id, 6F0A-A; Z-score, 9.0; sequence identity, 8%; rmsd value 3.5 Å), CmTDO (2NOX-B; 8.9; 13%; 2.8 Å), XcTDO (3BK9-B; 8.8; 9%; 2.8 Å), hTDO (5TI9-C; 8.3; 6%; 2.9 Å), DmTDO (4HKA-A; 7.9; 4%; 2.7 Å), hTDO (4PW8-H; 7.7; 6%; 3.0 Å), PrnB (2X67-A; 7.1; 15%; 3.1 Å) and hTDO (5TI9-A; 7.1; 5%; 3.0 Å). These data show that TDO and IDO are top ranks for structural similarity.

Tables

Table S1. The determined reciprocal relaxation times upon addition of ascorbate and •NO

	Fast (min)	Slow (min)		Fast (min)	Slow (min)
SfmD + ascorbate	1.92 ± 0.05	13.92 ± 0.48	SfmD, ascorbate + •NO	0.07 ± 0.00	7.83 ± 0.57
SfmD, 3-Me-L-Tyr + ascorbate	1.73 ± 0.03	10.60 ± 0.18	SfmD, 3-Me-L-Tyr, ascorbate + •NO	0.05 ± 0.00	8.02 ± 0.53
SfmD, L-Tyr + ascorbate	2.06 ± 0.05	19.91 ± 0.78	SfmD, L-Tyr, ascorbate + •NO	0.03 ± 0.00	10.28 ± 0.62
SfmD + 5,6-isopropylidene -L-ascorbate	3.30 ± 0.09	36.31 ± 1.16	N/A	N/A	N/A
C317S + ascorbate	8.75 ± 0.42	86.46 ± 5.62	C317S, ascorbate + •NO	4.07 ± 0.04	N/A
C317S, 3-Me-L-Tyr + ascorbate	10.55 ± 0.30	97.53 ± 4.52	C317S, 3-Me-L-Tyr, ascorbate + •NO	1.96 ± 0.07	10.81 ± 1.48

Table S2. X-ray data collection and phasing statistics for MAD (SeMet) structure

	SeMet substituted truncated SfmD		
Data Collection			
Space group		$P3_121$	
Cell dimensions			
a = b, c (Å)	59.29, 157.41	59.28, 157.38	59.30, 157.43
α, β, γ (°)		90, 90, 120	
	Peak	*Inflection*	*Remote*
Wavelength (Å)	0.97903	0.97920	0.97136
Resolution (Å)	50.00 – 2.20 (2.24 – 2.20)*	50.00 – 2.20 (2.24 – 2.20)	50.00 – 2.20 (2.24 – 2.20)
R_{sym} or R_{merge} (%)	15.2 (151.2)	14.5 (143.3)	14.4 (147.9)
$I/\sigma I$	21.6 (1.3)	23.4 (1.3)	22.9 (1.3)
Completeness (%)	99.5 (99.8)	99.4 (99.8)	99.6 (99.4)
Redundancy	18.4 (14.2)	18.4 (14.3)	18.4 (14.4)
FOM after RESOLVE		0.52	

*Values in parentheses are for the highest resolution shell.

Table S3. Primers used in this study. Mutagenesis primers for His274 and His313 were based on the codon-optimized DNA sequence of SfmD. Restriction enzyme sites and mutation sites are shown in underlined and bold, respectively.

Primers based on the original DNA sequence of SfmD				
Full-length	Forward	5′ –	TATGAATTCCATATGACGGCACCGGCCGAC	– 3′
(1 – 365)	Reverse	5′ –	AAGCTTTCACGAGGGTTCTCCCTG	– 3′
Truncated	Forward	5′ –	CATATGTACGTGGCCCAGGTGG	– 3′
(16 – 353)	Reverse	5′ –	AAGCTTTCAGAGCGCGCTCAGCC	– 3′
Mutagenesis primers based on the codon-optimized DNA sequence of SfmD				
H274A	Forward	5′ –	CACTGGCGTGAC**GCT**GAGGTGCTGATTAAA	– 3′
	Reverse	5′ –	TTTAATCAGCACCTC**AGC**GTCACGCCAGTG	– 3′
H274N	Forward	5′ –	CACTGGCGTGAC**AAC**GAGGTGCTGATTAAA	– 3′
	Reverse	5′ –	TTTAATCAGCACCTC**GTT**GTCACGCCAGTG	– 3′
H274Q	Forward	5′ –	CACTGGCGTGAC**CAA**GAGGTGCTGATTAAA	– 3′
	Reverse	5′ –	TTTAATCAGCACCTC**TTG**GTCACGCCAGTG	– 3′
H313A	Forward	5′ –	GACCTATGACAGC**GCC**ATTGGTGTTTGC	– 3′
	Reverse	5′ –	GCAAACACCAAT**GGC**GCTGTCATAGGTC	– 3′
H313N	Forward	5′ –	GACCTATGACAGC**AAC**ATTGGTGTTTGC	– 3′
	Reverse	5′ –	GCAAACACCAAT**GTT**GCTGTCATAGGTC	– 3′
H313Q	Forward	5′ –	GACCTATGACAGC**CAA**ATTGGTGTTTGC	– 3′
	Reverse	5′ –	GCAAACACCAAT**TTG**GCTGTCATAGGTC	– 3′
C317S	Forward	5′ –	GCCACATTGGTGTT**TCT**GGCCACTTTGTTG	– 3′
	Reverse	5′ –	CAACAAAGTGGCC**AGA**AACACCAATGTGGC	– 3′
C317A	Forward	5′ –	GCCACATTGGTGTT**GCC**GGCCACTTTGTTG	– 3′
	Reverse	5′ –	CAACAAAGTGGCC**GGC**AACACCAATGTGGC	– 3′

The codon-optimized DNA sequence of SfmD

ATGACCGCGCCGGCGGACACCGTTCATCCGGCGGGTCAGCCGGATTATGTGGCGCAAGTTGCGACCGTGCCGT
TTCGTCTGGGTCGTCCGGAGGAACTGCCGGGTACCCTGGATGAACTGCGTGCGGCGGTTAGCGCGCGTGCGGG
TGAAGCGGTTCGTGGCCTGAACCGTCCGGGTGCGCGTACCGATCTGGCGGCGCTGCTGGCGGCGACCGAGCGT
ACCCGTGCGGCGCTGGCGCCGGTTGGTGCGGGTCCGGTGGGTGATGATCCGAGCGAGAGCGAAGCGAACCGT
GACAACGATCTGGCGTTTGGCATCGTTCGTACCCGTGGTCCGGTTGCGGAACTGCTGGTTGACGCGGCGCTGGC
GGCGCTGGCGGGCATCCTGGAAGTGGCGGTTGATCGTGGTAGCGACCTGGAAGATGCGGCGTGGCAGCGTTTC
ATTGGTGGCTTTGATGCGCTGCTGGGTTGGCTGGCGGATCCGCACAGCGCGCCGCGTCCGGCGACCGTGCCGG
GTGCGGGTCCGGCGGGTCCGCCGGTTCATCAAGATGCGCTGCGTCGTTGGGTGCGTGGCCACCACGTTTTCATG
GTGCTGGCGCAAGGTTGCGCGCTGGCGACCGCGTGCCTGCGTGACAGCGCGGCGCGTGGTGATCTGCCGGGT
GCGGAGGCGAGCGCGGCGGCGGCGGAAGCGCTGATGCGTGGTTGCCAGGGTGCGCTGCTGTATGCGGGTGAT
GCGAACCGTGAGCAGTATAACGAACAAATCCGTCCGACCCTGATGCCGCCAGTTGCTCCGCCGAAGATGAGCGG
TCTGCACTGGCGTGAC**CAC**GAGGTGCTGATTAAAGAACTGGCGGGCAGCCGTGATGCGTGGGAGTGGCTGAGC
GCGCAAGGTAGCGAACGTCCGGCGACCTTCCGTGCGGCGCTGGCGGAGACCTATGACAGC**CAC**ATTGGTGTTT
GCGGCCACTTTGTTGGTGATCAAAGCCCGAGCCTGCTGGCGGCGCAAGGTAGCACCCGTAGCGCGGTGGGTGT
TATCGGCCAGTTTCGTAAGATTCGTCTGAGCGCGCTGCCGGAGCAACCGGCGACCCAGCAAGGTGAACCGAGCT
AA

Figures

Fig. S1. Validation of the single enantiomer of the synthetic substrate by NMR spectroscopy. Partial ^{1}H-NMR spectra ($CDCl_3$) of the amine TFA salt (top) and the (*R*)-Mosher amide derivative (bottom)

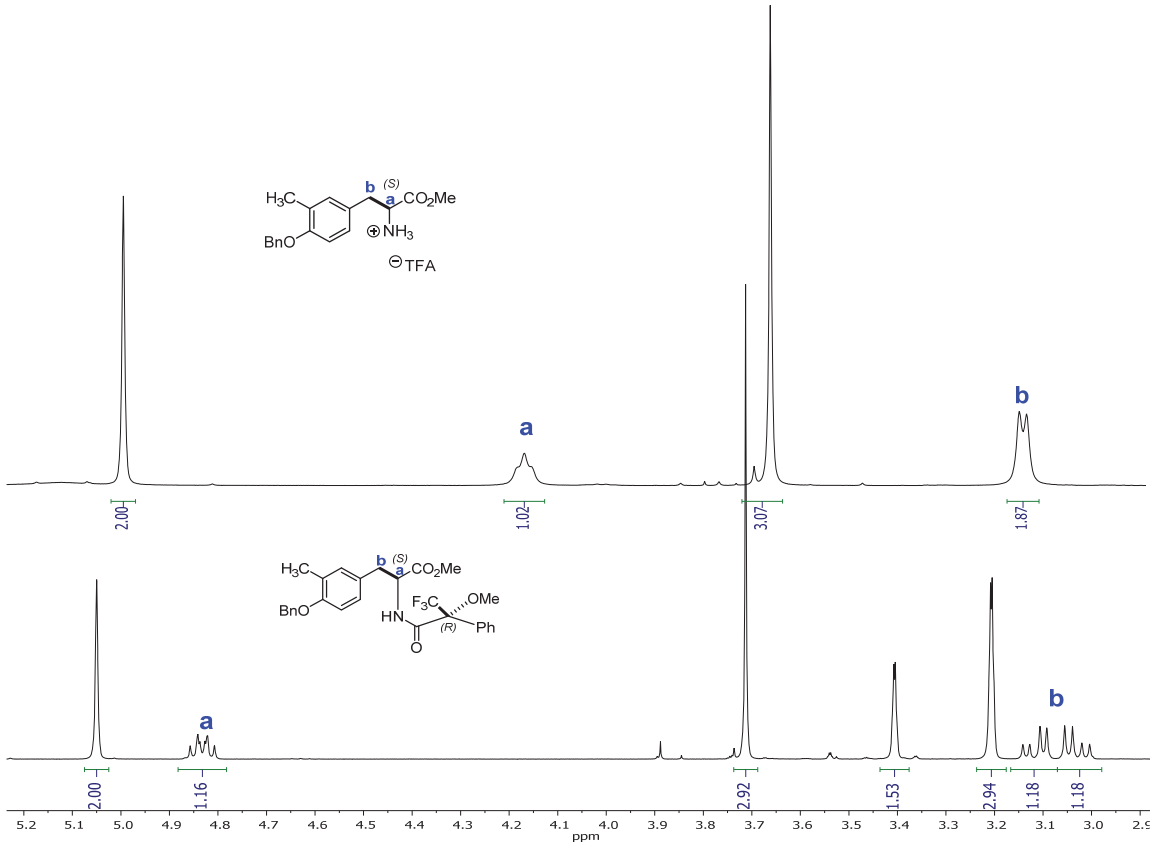

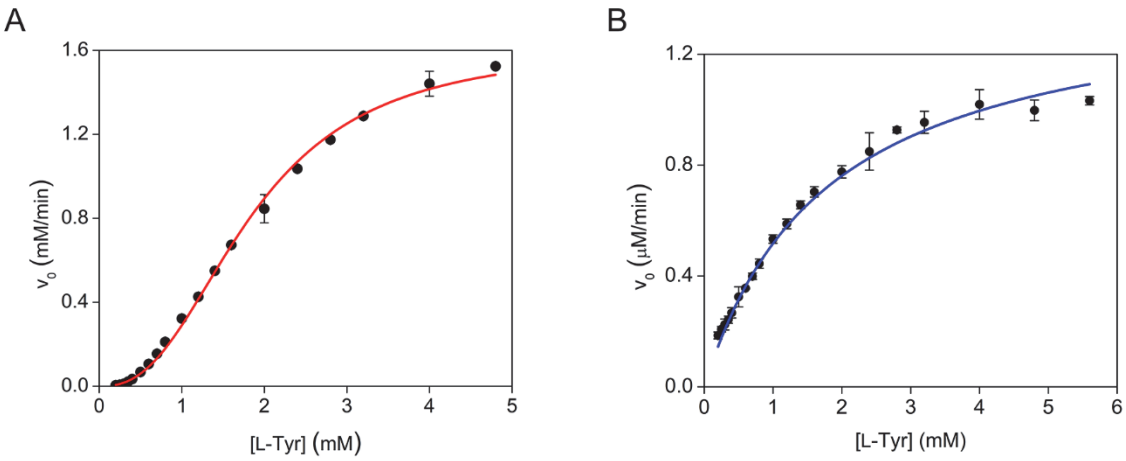

Fig. S2. Kinetic assay of SfmD in the hydroxylation of L-Tyr. (A) Assay with H_2O_2. The reaction was initiated by adding 4 mM of H_2O_2 to the mixture containing 50 μM enzyme and L-Tyr (0.2 – 4.8 mM) in pH 9.0 at 25 °C. The red curve shows the result of the nonlinear data fitting. (B) Assay with O_2 and ascorbate. The reaction was carried out with 50 μM enzyme, 20 mM ascorbate, and L-Tyr (0.2 – 5.6 mM) in pH 9.0 O_2-saturated buffer at 25 °C. The blue curve shows the result of the nonlinear data fitting.

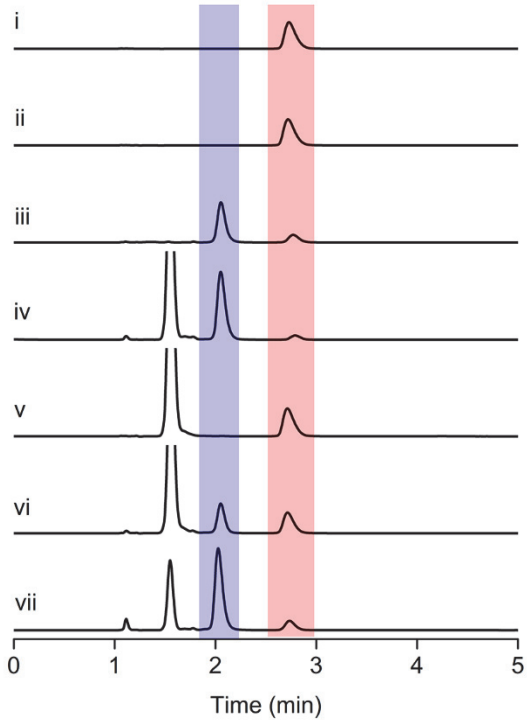

Fig. S3. HPLC analysis of the L-DOPA production through the hydroxylation reaction of L-Tyr catalyzed by SfmD. Absorbance at 280 nm was monitored and presented on the same scale. Peaks in the red and blue shaded boxes correspond to substrate and product, respectively. Ascorbate eluted at 1.7 min. (i) L-Tyr, (ii) enzyme and L-Tyr, (iii) enzyme, L-Tyr, and H_2O_2, (iv) enzyme, L-Tyr, H_2O_2, and ascorbate, (v) enzyme, L-Tyr, and ascorbate under anaerobic condition, (vi) enzyme, L-Tyr, and ascorbate under normoxic condition, and (vii) enzyme, L-Tyr, and ascorbate under O_2-saturated condition. The concentrations were: enzyme (SfmD, 30 μM), alternate substrate L-Tyr (1 mM), H_2O_2 (1 mM), and ascorbate (20 mM).

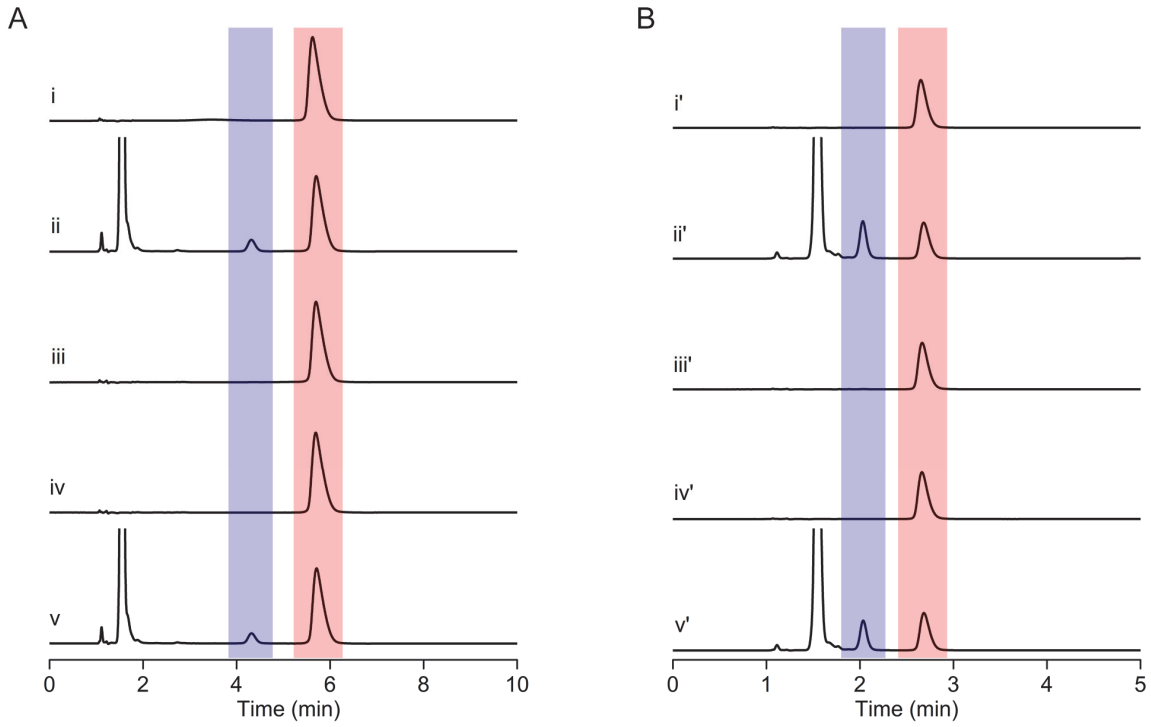

Fig. S4. HPLC analysis of the reaction catalyzed by SfmD in the presence of catalase. Absorbance at 280 nm was monitored. Peaks in the red and blue shaded boxes correspond to substrate and product, respectively. Ascorbate eluted at 1.7 min. (*A*) (i) 3-Me-L-Tyr, (ii) enzyme, 3-Me-L-Tyr, ascorbate, H_2O_2, and catalase (iii) enzyme, 3-Me-L-Tyr, H_2O_2, and catalase, (iv) enzyme, 3-Me-L-Tyr, and catalase, and (v) enzyme, 3-Me-L-Tyr, ascorbate, and catalase. (*B*) (i' – v') same as (i – v) except 3-Me-L-Tyr was replaced with L-Tyr. The concentrations were: enzyme (SfmD, 30 µM), substrate 3-Me-L-Tyr or L-Tyr (1 mM), H_2O_2 (1 mM), and ascorbate (20 mM), and catalase (10 µg).

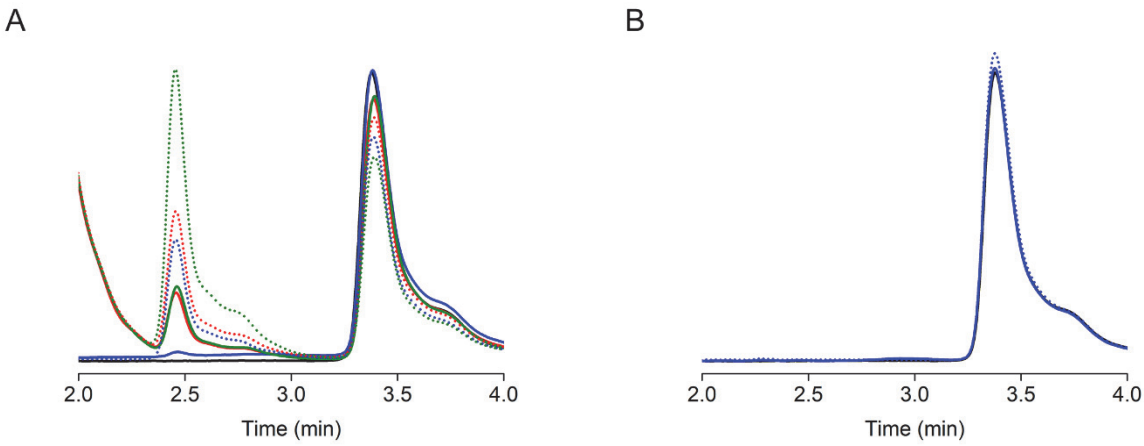

Fig. S5. The impact of the oxidation state of SfmD for oxidant selection in catalysis. (*A*) L-Tyr (black trace), Fe(III)-SfmD, L-Tyr, ascorbate (red), Fe(III)-SfmD, L-Tyr, H_2O_2 (blue), and Fe(III)-SfmD, L-Tyr, ascorbate, H_2O_2 (green) in the presence (solid line) and absence (dotted line) of catalase (20 µg), respectively. (*B*) L-Tyr (black), Fe(II)-SfmD, L-Tyr, H_2O_2 under normoxic (blue), and anaerobic condition (dotted blue), respectively. No catalase was included in the Fe(II)-SfmD experiments. The reactions were carried out using L-Tyr as a substrate in 100 µL volume for 2 hours. HPLC analysis was performed by monitoring absorbance at 280 nm. For better separation, 1% acetonitrile, 99% H_2O, 0.1% formic acid was used for isocratic elution. The concentrations were: enzyme (SfmD, 30 µM), L-Tyr (1 mM), H_2O_2 (1 mM), and sodium ascorbate (20 mM).

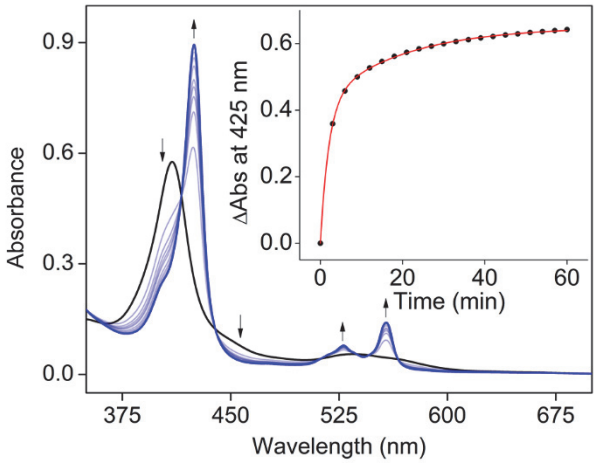

Fig. S6. UV-vis spectra of SfmD upon binding and reduction of ascorbate. The addition of ascorbate caused a red-shift of the Soret from 409 to 425 nm. Insets are the plots for changes at 425 nm as a function of time. Black trace: enzyme with L-Tyr; blue trace: enzyme with L-Tyr and ascorbate.

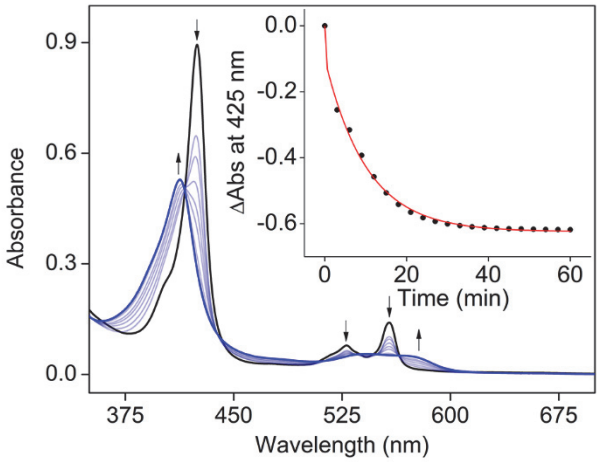

Fig. S7. UV-vis spectra of SfmD ferrous-nitrosyl complex. The ligand-free enzyme, L-Tyr, and ascorbate (black trace) and with the addition of •NO (blue trace). Addition of •NO caused a blue-shift of the Soret from 425 to 413 nm. Insets are the plots for changes at 425 nm as a function of time.

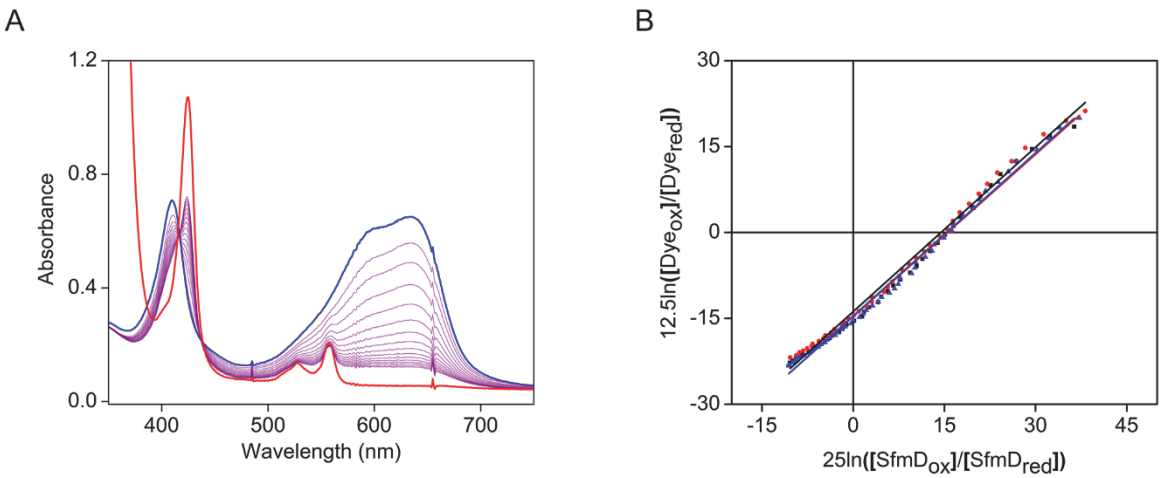

Fig. S8. Redox potential measurement of SfmD. (A) Representative spectra for the reduction of Nile Blue and SfmD. Blue trace represents the starting oxidized form of Nile Blue and SfmD mixture. Red trace is the fully reduced form with the addition of dithionite. (B) Nernst plots from three independent repeats of the measurement.

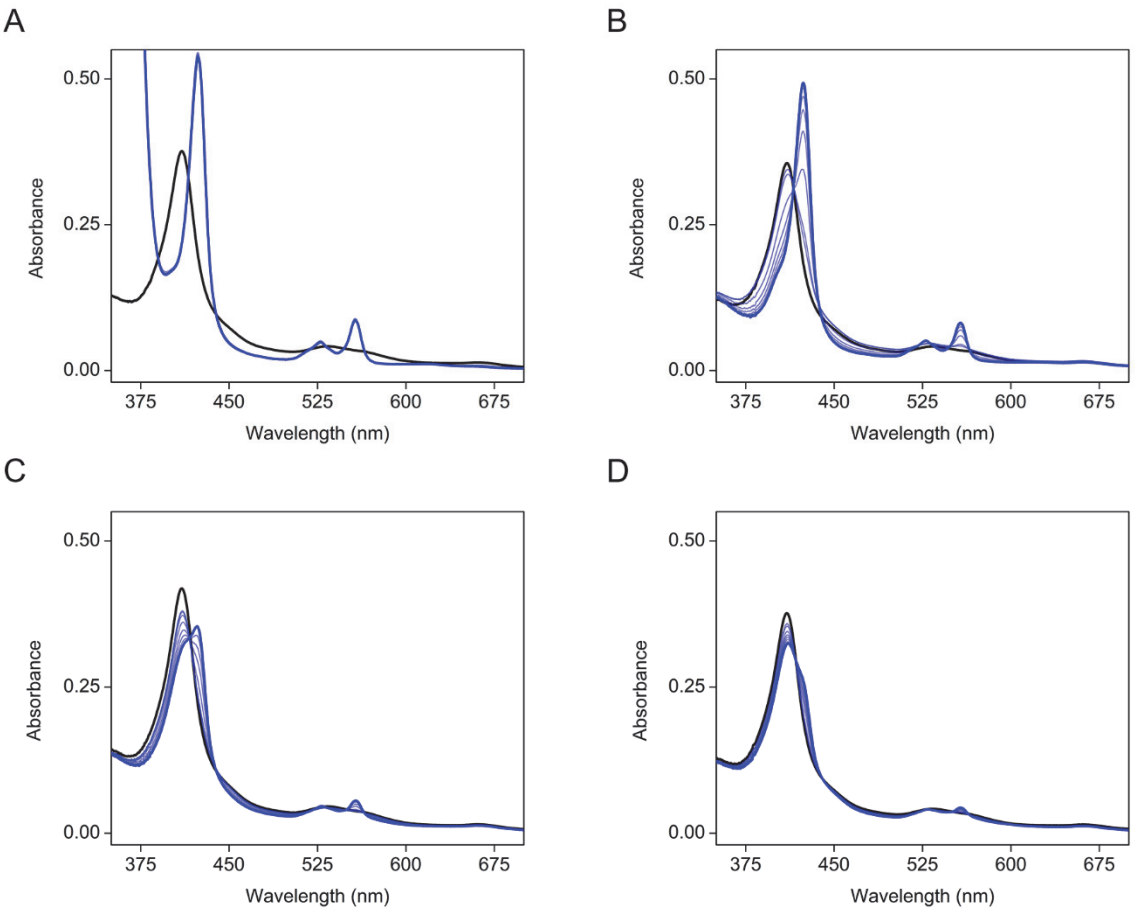

Fig. S9. Other reducing agents reduce SfmD. UV-vis spectra of SfmD reduction by other reducing agents were monitored for 1 hour and recorded in every 3 min. (A) dithionite, (B) DTT, (C) β-mercaptoethanol, and (D) TCEP. Black bold traces are the starting spectra before adding 20 mM reducing agent, and blue bold traces are the final spectra after 1 hour.

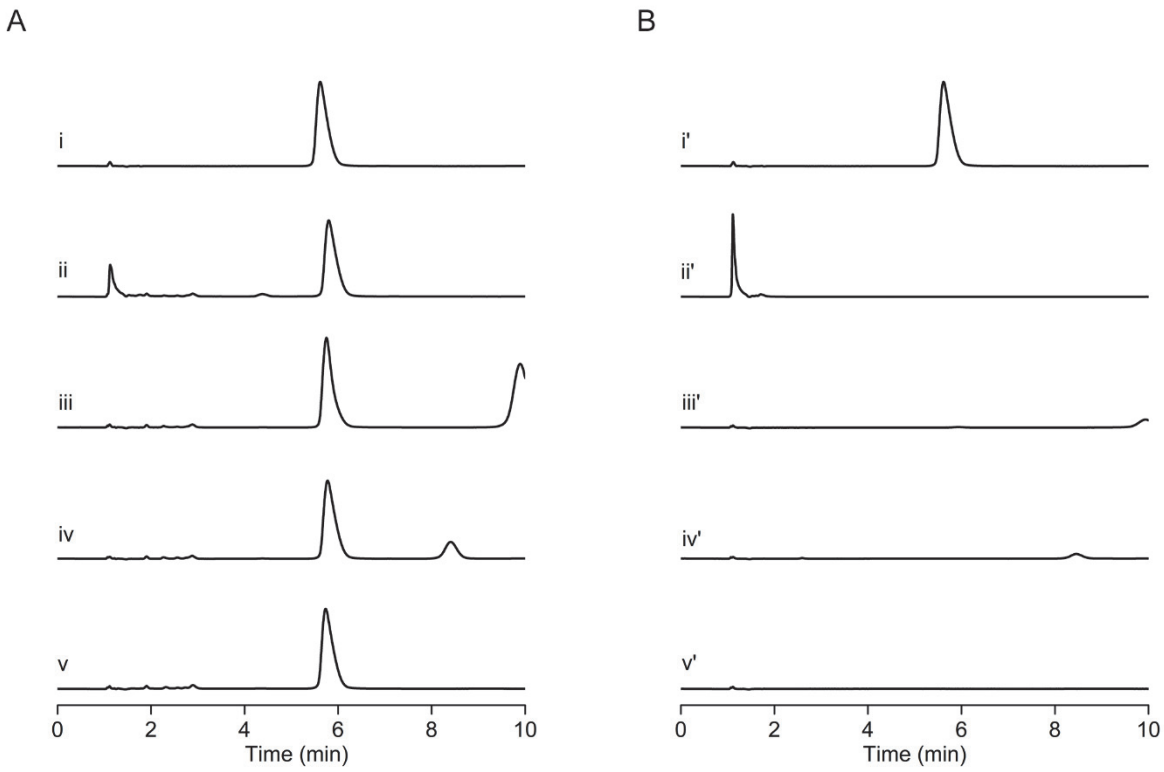

Fig. S10. **HPLC analysis of the reaction catalyzed by SfmD in the presence of other reducing agents**. (*A*) (i) 3-Me-L-Tyr, (ii) enzyme, 3-Me-L-Tyr, dithionite, (iii) enzyme, 3-Me-L-Tyr, dithiothreitol, (iv) enzyme, 3-Me-L-Tyr, β-mercaptoethanol, (v) enzyme, 3-Me-L-Tyr, TCEP, (*B*) (i') 3-Me-L-Tyr, (ii') dithionite, (iii') dithiothreitol, (iv') β-mercaptoethanol, and (v') TCEP. The concentrations were: enzyme (30 µM), substrate 3-Me-L-Tyr (1 mM), dithionite (20 mM), dithiothreitol (20 mM), β-mercaptoethanol (20 mM), and TCEP (20 mM).

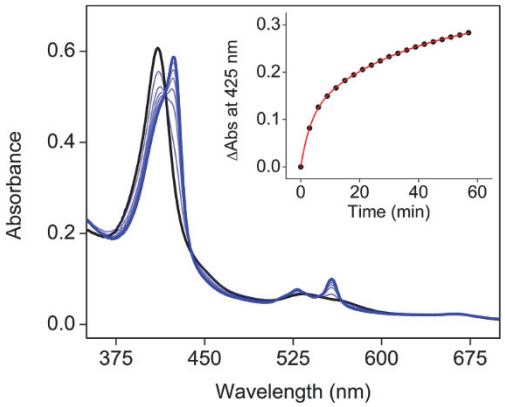

Fig. S11. 5,6-Isopropylidene-L-ascorbate reduces SfmD. UV-vis spectra showing the reduction of SfmD by 5,6-isopropylidene-L-ascorbate are presented: enzyme (black trace), and the enzyme with 5,6-isopropylidene-L-ascorbate (blue trace). The plots for changes at 425 nm as a function of time are shown in the inset.

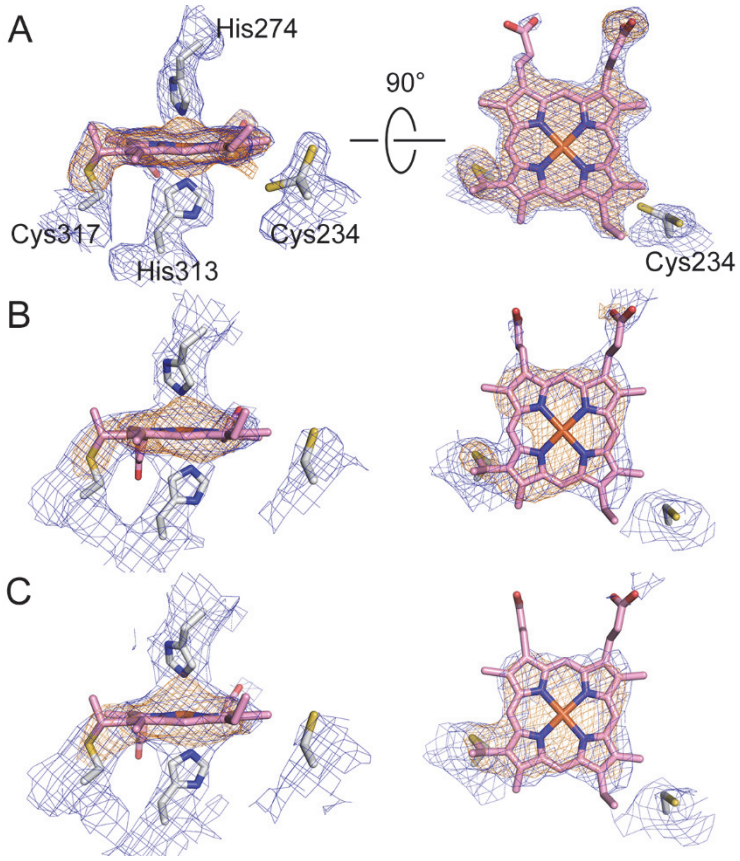

Fig. S12. Electron density maps for the novel heme attachment. 2F_o-F_c electron density maps from the final structural refinement are presented in blue contoured at 1 σ. (*A*) SfmD (PDB entry: 6VDP), (*B*) Partially reduced SfmD 'blue' intermediate (6VDZ), and (*C*) Partially reduced SfmD 'green' intermediate (6VE0). The omit F_o-F_c electron density maps for heme and Cys317 after simulated annealing are shown in orange contoured at 3 σ. Electron density maps are shown in two different orientations. For clarity, His274 and His313 were removed from top views.

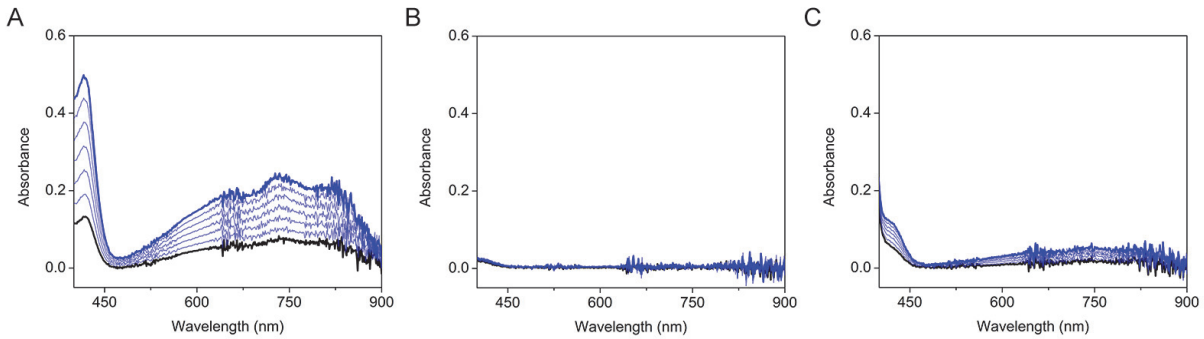

Fig. S13. Analysis of peroxidase activity of SfmD with the peroxidase substrate ABTS. Representative spectra of the SfmD peroxidase activity are shown as monitored by UV-visible spectroscopy for 1 min (from black trace to thick blue trace). (*A*) horseradish peroxidase (100 nM), ABTS (0.2 mM), and H_2O_2 (0.2 mM). (*B*) SfmD (100 nM), ABTS (0.2 mM), and H_2O_2 (0.2 mM). (*C*) SfmD (100 nM), ABTS (2 mM), and H_2O_2 (2 mM).

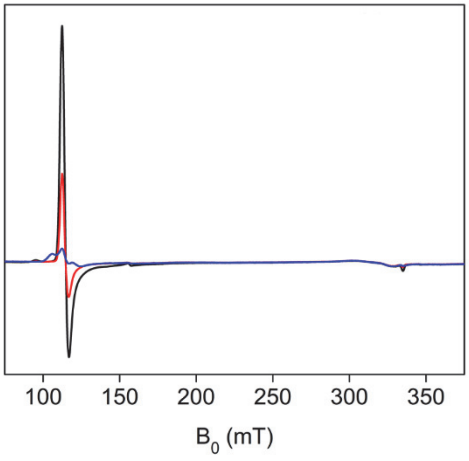

Fig. S14. Ferric heme reduction to ferrous by ascorbate in SfmD. EPR spectra of SfmD with 3-Me-L-Tyr (black), SfmD in complex with 3-Me-L-Tyr and added ascorbate for 30 min (red), and SfmD alone with ascorbate (blue) are shown. The concentrations were: 200 µM SfmD, 2.5 mM 3-Me-L-Tyr, and 50 mM ascorbate.

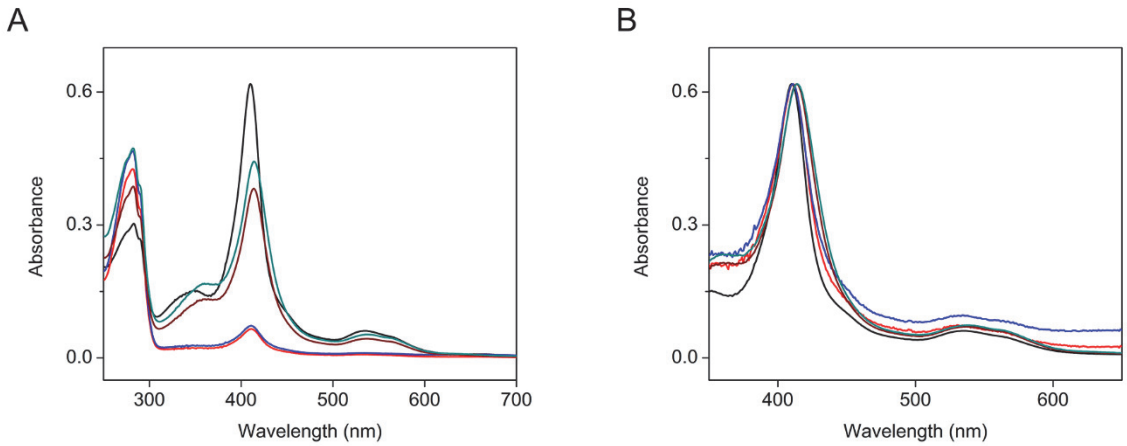

Fig. S15. The heme occupancy is significantly reduced in C317S and C318A SfmD variants. Cys317 was mutated to serine and alanine to remove the covalent linkage to heme. (A) UV-vis spectra of wild-type, C317S, and C317A enzymes and heme reconstituted C317S and C317A are shown. Black trace is wild-type, red and blue traces are C317S and C317A, respectively. Brown and dark green traces are C317S and C317A after heme reconstitution. (B) UV-vis spectra scaled to wild-type are presented for comparison. The color scheme is the same as in (A).

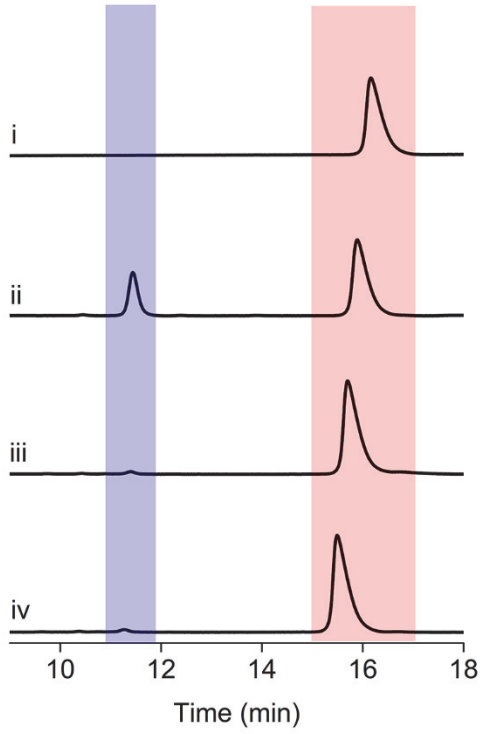

Fig. S16. C317S and C317A SfmD variants are catalytically inactive. The activity of C317S and C317A mutant enzymes were tested using HPLC. Absorbance at 280 nm was monitored and presented with the same scale. Peaks in the red and blue shaded boxes correspond to substrate and product, respectively. (i) 3-Me-L-Tyr, (ii) SfmD wild-type, 3-Me-L-Tyr, and ascorbate, (iii) SfmD C317S, 3-Me-L-Tyr, and ascorbate, (iv) SfmD C317A, 3-Me-L-Tyr, and ascorbate. No product formation was observed in mutant enzymes. The concentrations were: enzyme (SfmD wild-type and mutants, 30 µM), 3-Me-L-Tyr (1 mM), and ascorbate (20 mM).

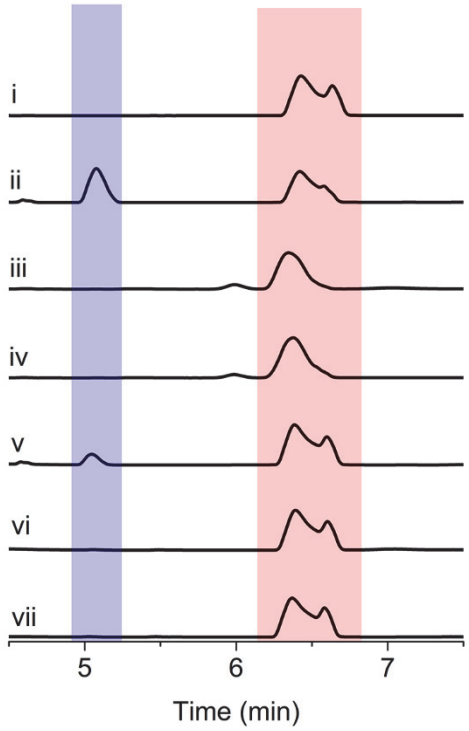

Fig. S17. Heme reconstituted C317S and C317A SfmD variants are catalytically inactive. The activity of heme reconstituted C317S and C317A mutant enzymes were tested using HPLC. Absorbance at 280 nm was monitored and presented with the same scale. Peaks in the red and blue shaded boxes correspond to substrate and product, respectively. (i) L-Tyr, (ii) SfmD wild-type, L-Tyr, and H_2O_2, (iii) SfmD C317S heme reconstituted, L-Tyr, and H_2O_2, (iv) SfmD C317A heme reconstituted, L-Tyr, and H_2O_2, (v) SfmD wild-type, L-Tyr, and ascorbate, (vi) SfmD C317S heme reconstituted, L-Tyr, and ascorbate, (vii) SfmD C317A heme reconstituted, L-Tyr, and ascorbate. No product formation was observed in the heme reconstituted mutant enzymes. The concentrations were: enzyme (SfmD wild-type and mutants, 25 µM), L-Tyr (1.6 mM), H_2O_2 (4 mM), and ascorbate (20 mM).

References

1. E. Augustyn, K. Finke, A. A. Zur, L. Hansen, N. Heeren, H. C. Chien, L. Lin, K. M. Giacomini, C. Colas, A. Schlessinger and A. A. Thomas, *Bioorg. Med. Chem. Lett.*, 2016, **26**, 2616-2621.
2. E. W. Schmidt, J. T. Nelson, and J. P. Fillmore, *Tetrahedron Letters*, 2004, **45**, 3921-3924.
3. M. C. Wood, D. C. Leitch, C. S. Yeung, J. A. Kozak and L. L. Schafer, *Angew. Chem. Int. Ed.*, 2007, **46**, 354-358.
4. G. D. Van Duyne, R. F. Standaert, P. A. Karplus, S. L. Schreiber and J. Clardy, *J. Mol. Biol.*, 1993, **229**, 105-124.
5. M. C. Tang, C. Y. Fu and G. L. Tang, *J. Biol. Chem.*, 2012, **287**, 5112-5121.
6. I. Barr and F. Guo, *Bio Protoc.*, 2015, **5**.
7. I. Efimov, G. Parkin, E. S. Millett, J. Glenday, C. K. Chan, H. Weedon, H. Randhawa, J. Basran and E. L. Raven, *FEBS Lett.*, 2014, **588**, 701-704.
8. Z. Otwinowski and W. Minor, *Methods Enzymol.*, 1997, **276**, 307-326.
9. T. C. Terwilliger and J. Berendzen, *Acta Crystallogr. D Biol. Crystallogr.*, 1999, **55**, 849-861.
10. T. C. Terwilliger, *Acta Crystallogr. D Biol. Crystallogr.*, 2000, **56**, 965-972.
11. T. C. Terwilliger, *Acta Crystallogr. D Biol. Crystallogr.*, 2003, **59**, 38-44.
12. P. Emsley, B. Lohkamp, W. G. Scott and K. Cowtan, *Acta Crystallogr. D Biol. Crystallogr.*, 2010, **66**, 486-501.
13. P. D. Adams, P. V. Afonine, G. Bunkoczi, V. B. Chen, I. W. Davis, N. Echols, J. J. Headd, L. W. Hung, G. J. Kapral, R. W. Grosse-Kunstleve, A. J. McCoy, N. W. Moriarty, R. Oeffner, R. J. Read, D. C. Richardson, J. S. Richardson, T. C. Terwilliger and P. H. Zwart, *Acta Crystallogr. D Biol. Crystallogr.*, 2010, **66**, 213-221.
14. F. Sievers, A. Wilm, D. Dineen, T. J. Gibson, K. Karplus, W. Li, R. Lopez, H. McWilliam, M. Remmert, J. Soding, J. D. Thompson and D. G. Higgins, *Mol. Syst. Biol.*, 2011, **7**, 539.
15. X. Robert and P. Gouet, *Nucleic Acids Res.*, 2014, **42**, W320-324.
16. S. McNicholas, E. Potterton, K. S. Wilson, and M. E. Noble, *Acta Crystallogr. D Biol. Crystallogr.*, 2011, **67**, 386-394.
17. T. D. Goddard, C. C. Huang, E. C. Meng, E. F. Pettersen, G. S. Couch, J. H. Morris and T. E. Ferrin, *Protein Sci.*, 2018, **27**, 14-25.
18. L. A. Kelley, S. Mezulis, C. M. Yates, M. N. Wass and M. J. Sternberg, *Nat. Protoc.*, 2015, **10**, 845-858.
19. L. Holm and L. M. Laakso, *Nucleic Acids Res.*, 2016, **44**, W351-W355.